Structure of the noncubic phase in the ferroelectric state of Pr-substituted $SrTiO_3$

Rohini Garg,[1] Anatoliy Senyshyn,[2] Hans Boysen,[3] and Rajeev Ranjan[1,*]
[1]*Department of Materials Engineering, Indian Institute of Science, Bangalore-560012, India*
[2]*Institute for Materials Science, Darmstadt University of Technology, Petersenstrasse 23, D-64287 Darmstadt, Germany*
[3]*Department fur Geo-und Umweltwissenschaften, Sektion Kristallographie, Ludwig Maximilians Universität, Am Coulombwall 1, 85748 Garching, München, Germany*
(Received 11 February 2009; revised manuscript received 26 March 2009; published 29 April 2009)

$Sr_{1-x}Pr_xTiO_3$ has recently been shown to exhibit ferroelectricity at room temperature. In this paper powder x-ray and neutron-diffraction patterns of this system at room temperature have been analyzed to show that the system exhibits cubic (Pm-3m) structure for $x \leq 0.05$ and tetragonal ($I4/mcm$) for $x > 0.05$. The redundancy of the noncentrosymmetric structural model ($I4cm$) in the ferroelectric state suggests the absence of long-range ordered ferroelectric domains and supports the relaxor ferroelectric model for this system.

DOI: 10.1103/PhysRevB.79.144122 PACS number(s): 77.84.Dy, 61.50.Ks, 77.80.Bh

I. INTRODUCTION

$SrTiO_3$ (ST) is one of the very few compounds in the perovskite family which exhibits simple-cubic structure at room temperature. For many years, it has been the model system for understanding the physics of soft phonon driven structural phase transitions in solids.[1,2] The system has two soft modes. One of them is associated with the R point of the cubic Brillouin zone which, on cooling, freezes at 105 K thereby leading to a cubic (Pm-$3m$) to tetragonal ($I4/mcm$) structural phase transition. The other soft mode is associated with the zone center of the Brillouin zone. The condensation of this mode is responsible for occurrence of ferroelectric transitions in the classical ferroelectrics such as $BaTiO_3$ and $PbTiO_3$. However, for ST condensation of this ferroelectric mode never takes place down to the lowest temperature, presumably due to high-energy ground-state quantum fluctuations associated with the lattice degree of freedom.[3] The system has accordingly been designated as quantum paraelectric[3] and incipient ferroelectric.[4] The ferroelectric state can, however, be stabilized at low temperatures on application of external stress,[5] electric field,[6,7] chemical,[8–10] and isotopic[11] substitutions. Chemical substitutions lead to interesting changes in the polar behavior of ST. Bednorz and Muller[8] first reported quantum ferroelectricity in Ca-substituted ST with maximum $T_c \sim 35$ K. Later, it was shown that further Ca substitution drives the system toward an antiferroelectric ground state with a structure similar to that of $NaNbO_3$ at room temperature.[12] Occurrence of quantum ferroelectric transition and gradual stabilization of a normal ferroelectric state was also reported for Ba and Pb substituted ST.[9,10] This is not very surprising in view of the fact that $BaTiO_3$ and $PbTiO_3$ are classical ferroelectric systems at room temperature and above. Of the hetrovalent substitutions, Bi substitution has been reported to stabilize ferroelectricity up to ~100 K for 4 mol % of Bi at the Sr site.[13] Studies pertaining to stabilization of ferroelectric state in ST above room temperature have also been made. Pertsev *et al.*[14] have predicted that by tuning biaxial strain the ferroelectric transition temperature of ST can be increased significantly. This was subsequently realized for thin ST film grown on $DyScO_3$ substrate.[15] For bulk case, Kornev and Bellaiche have predicted that ST can become ferroelectric at very high pressure.[16] Another interesting development was reported by Duran *et al.*[17] for Pr-substituted ST system. The authors reported peaks in the relative permittivities of $Sr_{1-x}Pr_xTiO_3$ (SPT) for $x=0.025$, 0.05 and 0.075 around 500 K and polarization-electric field hysteresis loop, characteristic of a ferroelectric state, at room temperature. Subsequently, features of relaxor behavior and development of spontaneous lattice strain near the dielectric anomaly temperature were also reported for $x=0.05$.[18,19] More recently, Duran *et al.* reported evidence of symmetry breaking associated with the dielectric anomaly for a higher composition, $x=0.15$, and claimed that the structure of the ferroelectric state at room temperature of $Sr_{0.85}Pr_{0.15}TiO_3$ is similar to that of the tetragonal structure of $BaTiO_3/PbTiO_3$.[20] The authors reported a weak anomaly at ~455 K in differential thermal analysis (DTA) data. This temperature is ~50 K lower than the temperature (515 K) corresponding to the peak in the relative permittivity.[20] Since it is well known that for a normal ferroelectric phase transition the Curie point and the structural transition temperatures almost coincide within a few degrees, the interpretation of 455 K anomaly in terms of ferroelectric-paraelectric transition, reported in Ref. 20, needs careful examination. The occurrence of symmetry breaking well below the dielectric anomaly temperature is, however, known to occur in some of the relaxor ferroelectrics.[21,22] In this paper we have examined the structure of the SPT using a combination of x-ray and neutron powder-diffraction techniques to settle this issue. Our analysis revealed that the tetragonal structure of SPT is not of ferroelectric $BaTiO_3$ type proposed earlier, but corresponds to an antiferrodistortive phase consisting of out-of-phase tilted octahedra without any noticeable signature of polar distortion.

II. EXPERIMENTAL

SPT specimens were prepared by solid-state reaction of $SrCO_3$, Pr_6O_{11}, and TiO_2. The powders were thoroughly mixed in a planetary ball mill with agate bowls and balls. Acetone was used as the mixing medium. Calcination was done at 1100 °C for 3 h. Uniaxially pressed pellets of the

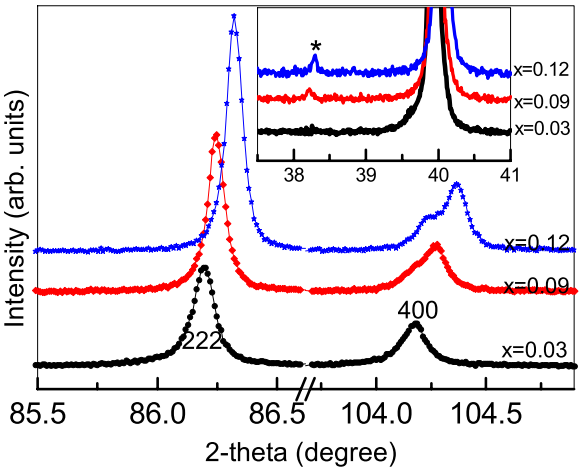

FIG. 1. (Color online) Magnified plot of pseudocubic 222 and 400 x-ray Bragg profiles of $Sr_{1-x}Pr_xTiO_3$ (x=0.03, 0.09, 0.12).

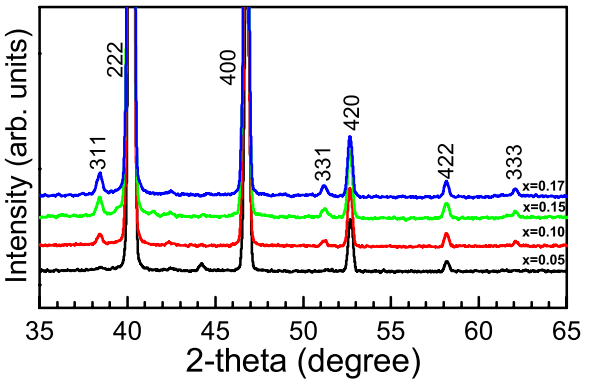

FIG. 2. (Color online) Part of the neutron powder-diffraction patterns of $Sr_{1-x}Pr_xTiO_3$ for x=0.05, 0.10, 0.15, and 0.17. The indices are with respect to a doubled pseudocubic axis (see text).

calcined powders were sintered at 1300 °C for 4 h. X-ray diffraction was performed on Bruker diffractometer using Cu $K\alpha$ radiation. A double monochromator assembly was used to eliminate the $K\alpha_2$ component and improved the resolution significantly, thereby enabling us to resolve the weak splitting of the Bragg peaks and to determine the nature of the distortion of the cubic lattice. Neutron powder-diffraction experiment was carried out at the SPODI diffractometer at FRM II, Germany using a wavelength of 1.548 Å. "Fullprof" was used for Rietveld refienement.[23]

III. RESULTS AND DISCUSSION

A. Room-temperature structure: X-ray diffraction study

Figure 1 shows a magnified view of the pseudocubic 222 and 400 XRD Bragg profiles of three compositions x=0.03, 0.09, and 0.12. For x=0.03, both the peaks are singlet and hence the average structure is cubic. This is in conformity with the fact that x=0.05 was also reported to exhibit a cubic structure.[19] The width of the peaks are, however, slightly larger than the instrumental resolution suggesting presence of local deviations from the cubic symmetry. For x=0.09 and 0.12, the 222 remains a singlet, while the 400 splits into two, with an intensity ratio 1:2, suggesting tetragonal distortion of the cubic lattice. The simplest structure consistent with this distortion is of the type known for $BaTiO_3$ and $PbTiO_3$ at room temperature. Duran *et al.* have reported in Ref. 20 a similar type of splitting of the 200 pseudocubic Bragg profile of x=0.15 and have concluded $BaTiO_3$ type tetragonal (space group $P4mm$) structure for x=0.15. A careful look, however, revealed presence of a weak reflection near 2θ =38°, the intensity of which grows up with increasing Pr content, as shown in the inset of Fig. 1. With respect to a doubled pseudocubic perovskite cell ($2a_p \times 2b_p \times 2c_p$), the weak reflection is indexed as 311. This suggests that the weak reflection is representative of a superlattice structure, with doubling of the pseudocubic cell in all the three pseudocubic directions.[24–26] This clearly ruled out the possibility of a $BaTiO_3$ type structure at room temperature proposed in Ref. 20. In general, cell doubling can occur either by 1:1 chemical ordering of cations in neighboring lattice planes of the pseudocubic lattice or by tilting of the anion octahedra. The 1: 1 ordering in the present case is extremely unlikely as the Pr content is significantly less than 0.50. For a Ca substituted ST system, which exhibits complete solid solubility, it has been shown that even for $Sr_{0.5}Ca_{0.5}TiO_3$ Sr and Ca ions does not exhibit chemical ordering and rather prefers random solution.[27] The superlattice reflections in the powder pattern of Ca-substituted ST could be explained only in terms of octahedral tilts.[27] A systematic classification of different types of tilted octahedral structures in perovskites is given by Glazer.[24,25] For small magnitude of tilt, the intensity of the superlattice reflections is weak in x-ray diffraction patterns due to relatively weak scattering of x rays by the low Z oxygen as compared to other elements in the structure. As a result, in such situations, reliable structure analysis is extremely difficult with x-ray powder-diffraction data.[28–30] This limitation is overcome when use is made of neutron diffraction. This was nicely demonstrated for the case of the $PbZr_{0.52}Ti_{0.48}O_3$ at low temperature for which the correct space group at low temperature was found to be Cc instead of Cm.[29,30]

B. Room-temperature structure: Neutron-diffraction study

Figure 2 shows a part of the neutron powder-diffraction patterns of some selected compositions of $Sr_{1-x}Pr_xTiO_3$. Because of the comparatively low resolution of the neutron powder diffractometer we did not find splitting in any of the Bragg peaks. The Bragg peaks in this figure are indexed with respect to a doubled pseudocubic perovskite cell. The all-odd index reflections, in this scheme of indexing, correspond to the superlattice reflections. For x=0.05, no superlattice reflections are visible and hence the structure of this composition is cubic. In contrast to the x-ray diffraction patterns, the neutron-diffraction patterns contain more than one superlattice reflections of the all-odd type. A perusal of Glazer's classification scheme suggests that the only structure that can explain the tetragonal distortion of the cubic lattice along with the presence of all-odd superlattice reflections in the diffraction pattern is consistent with the $a^0a^0c^-$ tilt

TABLE I. Structural parameters of $Sr_{1-x}Pr_xTiO_3$ at 300 K obtained after refinement with $I4/mcm$ space group.

	$Sr_{1-x}Pr_xTiO_3$			
Refinable parameters	$x=0.10$	$x=0.13$	$x=0.15$	$x=0.17$
a (Å)	5.5181(2)	5.5183(2)	5.5183(2)	5.5171(2)
c (Å)	7.8084(4)	7.8107(4)	7.8075(6)	7.8106(4)
$B_{Sr/Pr}$ (Å^2)	0.60(3)	0.66(3)	0.68(3)	0.68(3)
B_{Ti} (Å^2)	0.56(3)	0.34(3)	0.53(3)	0.53(3)
B_{O1} (Å^2)	0.30(4)	0.76(9)	0.53(5)	0.53(5)
x_{O2} (Å)	0.2384(2)	0.2377(2)	0.2363(2)	0.2352(2)
y_{O2} (Å)	0.2616(2)	0.2623(2)	0.2637(2)	0.2648(2)
B_{O2} (Å^2)	0.86(3)	0.67(4)	0.83(3)	0.88(3)
	$R_e=2.50$	$R_e=3.73$	$R_e=2.20$	$R_e=2.27$
	$R_{wp}=6.29$	$R_{wp}=6.10$	$R_{wp}=6.15$	$R_{wp}=6.08$

system.[24–26] This structure consists of neighboring oxygen octahedra along the c axis of the tetragonal cell rotated out of phase. Pure ST exhibit this structure (space group $I4/mcm$) below 105 K. Rietveld refinement was accordingly carried out as per this structural model for all the compositions exhibiting superlattice reflections in the neutron-diffraction patterns. The tetragonal lattice parameters of this unit cell ($a_t=b_t, c_t$) is related to the pseudocubic lattice parameters ($a_p=b_p$, c_p) as $a_t=\sqrt{2}a_p, c_t=2c_p$. The asymmetric unit of the structure consists of one Sr/Pr at (0, 0.5, 0.25), one Ti at (0, 0, 0), one oxygen O1 at (0, 0, 0.25) and another oxygen O2 at (0.25−Δ, 0.25+Δ, 0). Thus, apart from the thermal parameters, this structure has only three structural variables, two lattice parameters and one coordinate. The octahedral tilt angle, φ, (out-of-phase tilted neighboring oxygen octahedra along the c axis of the tetragonal cell) can be determined from the relation $\tan\varphi=4\Delta$. Table I lists the refined structural parameters for the different compositions. Figure 3 shows a Rietveld plot of a representative composition ($x=0.15$) after refinement with this structural model. The variation in the pseudocubic lattice parameters a_p, c_p, pseudocubic volume (v_p) and octahedral tilt angle with compositions is shown in Fig. 4. It is evident from this figure that the tetragonality, which is a measure of the difference between the a_p and c_p, and the tilt angle tend to vanish near $x=0.05$,

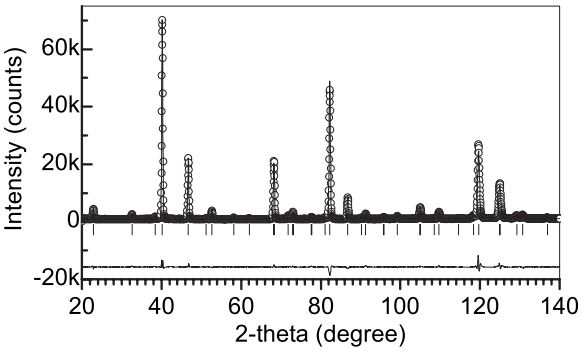

FIG. 3. Rietveld plot of the neutron powder-diffraction pattern of $Sr_{0.85}Pr_{0.15}TiO_3$ after refinement with $I4/mcm$ space group.

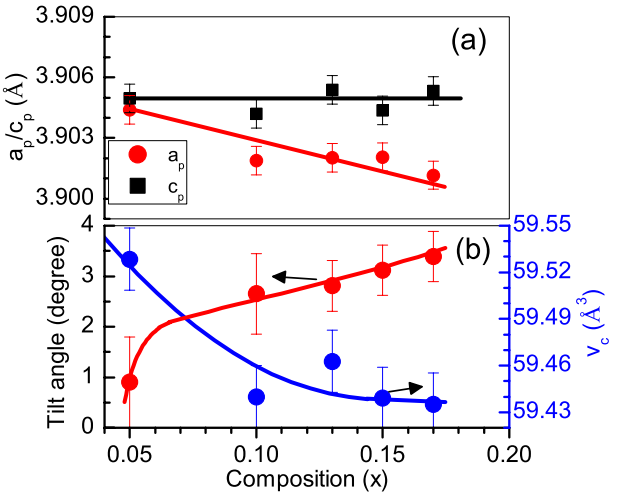

FIG. 4. (Color online) Variation in (a) pseudocubic lattice parameters and (b) octahedral tilt angle and pseudocubic volume with composition. The solid lines are guide to the eyes.

suggesting $x=0.05$ to be the boundary composition that separates the tetragonal ($I4/mcm$) and the cubic ($Pm\text{-}3m$) structures at room temperature. As mentioned above, the cubic-tetragonal antiferrodistortive (AFD) phase-transition temperature of ST is 105 K. This temperature is known to increase when the chemical substitution involves smaller sized ions (such as Ca^{+2}) as compared to Sr^{+2}.[31] Since the size of the Pr ions, either in the +3 or +4 oxidation state is smaller than that of Sr^{+2}, the increase in the AFD transition temperature with substitution of Pr at the A site is therefore anticipated.

C. Centrosymmetric versus noncentrosymmetric structural models for 300 K

The $I4/mcm$ structure is centrosymmetric and hence is incompatible with a long-range ordered ferroelectric state. We, therefore, also considered the corresponding noncentrosymmetric space group, $I4cm$ which can allow the octahedral tilt of the type $a^0a^0c^-$, mentioned above, to coexist with polar (ferroelectric) distortion. Except for the possibility of the z coordinates of the atom to vary, the asymmetric unit of the $I4cm$ structure is the same as that of the $I4/mcm$. For

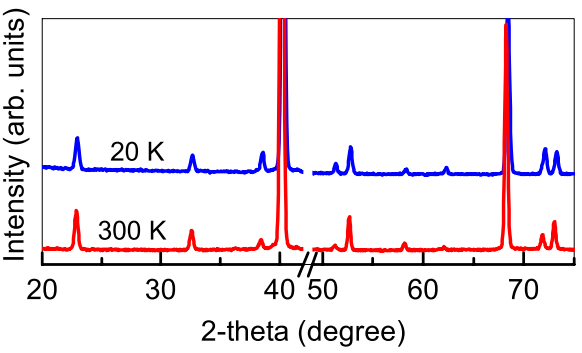

FIG. 5. (Color online) Part of the neutron powder-diffraction pattern of $x=0.15$ at 300 and 20 K.

TABLE II. Comparison of the structural parameters of $Sr_{0.85}Pr_{0.15}TiO_3$ at 300 K obtained with $I4/mcm$ and $I4cm$ space groups.

	$I4/mcm$				$I4cm$			
Atoms	a=5.5183(2) Å		c=7.8075(6) Å		a=5.5178(2) Å		c=7.8089(6) Å	
	x	y	z	B(Å^2)	x	y	z	B(Å^2)
Sr/Pr	0	0.5	0.25	0.61(2)	0	0.5	0.25	0.26 (9)
Ti	0	0	0	0.54(3)	0	0	0.011(2)	0.7(2)
O1	0	0	0.25	0.37(4)	0	0	0.262(5)	0.7(2)
O2	0.2363(2)	0.2637(2)	0	0.86(3)	0.2368(2)	0.2631(2)	−0.001(2)	0.68(6)
		R_{wp}:6.15	R_{exp}:2.20		R_{wp}:6.23	R_{exp}:2.20		

sake of reference, we fixed the coordinates of Sr/Pr at 0, 0.5, 0.25 and varied the z coordinates of the remaining atoms (Ti, O1, and O2) during the refinement. However, we noted no improvement in the fit. In fact the goodness of fit parameter was found to oscillate with the progress of the refinement cycle, thereby suggesting unstable solution with the $I4cm$ structural model. The refined coordinates and other structural parameters of x=0.15, corresponding to the minimum value of the goodness of fit, are shown in Table II for comparison. Since the refinement could not converge smoothly, and even the lowest value of the goodness of fit parameter obtained with the $I4cm$ model is still higher than that of $I4cm$, the changes in the z coordinates of Ti, O1, and O2 with respect to that of the corresponding values in the $I4/mcm$ model is of no significance. The redundancy of the structural model based on the $I4cm$ space group suggests that the structure of SPT for $x>0.05$ does not involve long-range ferroelectric distortion and hence the ferroelectric state below the dielectric anomaly temperature (~515 K) does not involve breaking of inversion symmetry at the global scale. In this scenario, the ferroelectric state in the SPT system is most likely to occur due to freezing of polar clusters below the dielectric peak temperature as in relaxor ferroelectrics.[21,22] It may be mentioned that the dielectric anomalies and the electric field-polarization hysteresis loop have as well been reported for compositions exhibiting the cubic (Pm-3m) structure ($x \leq 0.05$) at room temperature. Thus, though the average crystal structure changes from cubic (Pm-3m) to tetragonal ($I4/mcm$) on increasing the Pr content beyond x=0.05, the fact that the system exhibits ferroelectricity at room temperature for compositions below and above x=0.05 is indicative of decoupled nature of the ferroelectric state and the global structure in this system.

Further, since the antiferrodistortive phase (tetragonal, $I4/mcm$) is already stabilized at room temperature for x =0.15, the corresponding condensation of the zone-boundary soft mode must necessarily have taken place above room temperature. Hence, in contrast to the conjecture made in Ref. 20, our results suggest that the anomaly in the thermal measurements at 455 K, and not that at 105 K, is most likely to be representing the AFD transition.

D. Structure at low temperature

Having shown above that the structural model consistent with a global ferroelectric distortion leads to unstable refinement at 300 K, we also analyzed the structure of $Sr_{0.85}Pr_{0.15}TiO_3$ well below room temperature to determine if any noticeable ferroelectric distortion develops in the system or not. Figure 5 compares the neutron powder-diffraction patterns at 300 and 20 K in limited 2θ ranges. It is apparent from this figure that the only change in the pattern of 20 K is the enhancement of the relative intensities of the already existing superlattice reflections (at room temperature). The absence of new reflections at 20 K suggests that the structural distortion observed at 300 K is more or less intact down to 20 K. Since 20 K is sufficiently well below the dielectric anomaly temperature (~515 K) reported for this composition, it may be anticipated that the system may acquire some degree of global ferroelectric distortion as in some of the relaxor ferroelectric systems.[21,22] Rietveld refinement was therefore carried out with both centrosymmetric ($I4/mcm$) and noncentrosymmetric ($I4cm$) structural models. Unlike for the data corresponding to 300 K which led to large oscillations in the goodness of fit parameter in successive cycles when refined with $I4cm$ model, the refinement converged smoothly for the 20 K data with the $I4cm$ model. The refined structural parameters at 20 K with both the structural models are given in Table III. A comparison with the corresponding data in Table III suggests that the x and y fractional coordinates of O2 have further departed from their ideal cubic value ($x=y=0.25$) as compared to 300 K, suggesting further increase in the octahedral tilt angle on cooling down to 20 K. This is also consistent with the fact that the cell volume has decreased from 237.75(2) Å^3 at 300 K to 236.38(1) Å^3 at 20 K. As expected, the atomic displacement parameters have decreased compared to their respective values at 300 K. It is worth noting that although the tetragonal a parameter has decreased, the c parameter has slightly increased on cooling (from 7.8075(6) Å at 300 K to 7.8119(1) Å at 20 K). Since the c axis is also the polar axis of the $I4cm$ structure, it is tempting to interpret the small increase in its value on cooling to onset of a global ferroelectric ordering below room temperature. However, the significance of the polar distortion, as obtained with the $I4cm$ model, and manifested in terms of the deviations of the z coordinates from their respective ideal values (corresponding to the centrosymmetric $I4/mcm$ model) is still debatable since the goodness of the fit parameter (R_{wp}) is nearly same for both $I4/mcm$ (R_{wp} =4.40) and $I4cm$ (R_{wp}=4.38) models.

TABLE III. Comparison of the structural parameters of $Sr_{0.85}Pr_{0.15}TiO_3$ at 20 K obtained with $I4/mcm$ and $I4cm$ space groups.

	$I4/mcm$				$I4cm$			
Atoms	a=5.5008(1) Å		c=7.8119(1) Å		a=5.5008(1) Å		c=7.8119(1) Å	
	x	y	z	B(Å^2)	x	y	z	B(Å^2)
Sr/Pr	0	0.5	0.25	0.24(2)	0	0.5	0.25	0.23 (2)
Ti	0	0	0	0.14(3)	0	0	−0.005(2)	0.15(4)
O1	0	0	0.25	0.28(3)	0	0	0.246 (1)	0.30(4)
O2	0.2289(1)	0.2711(1)	0	0.40(2)	0.2290(1)	0.2710(1)	0.002(1)	0.38(2)
	R_{wp}:4.40	R_{exp}:2.16			R_{wp}:4.38	R_{exp}:2.16		

IV. CONCLUSIONS

In conclusion, a combination of high-resolution XRD and neutron-diffraction data resolved the issues related to the crystal structure and the ferroelectric state in $Sr_{1-x}Pr_xTiO_3$. The room-temperature crystal structure changes from cubic (Pm-$3m$) to tetragonal ($I4/mcm$) around $x \sim 0.05$. A temperature-dependent study for x=0.15, suggested that there is no further change in the structure on cooling down to 20 K. A comparative structural analysis between the nonpolar structure ($I4/mcm$) and a polar structure ($I4cm$) for x =0.15 revealed that the average global structure remains centrosymmetric tetragonal ($I4/mcm$) down to 20 K. A slight increase in the c parameter is however noticed on cooling.

The observation of the ferroelectric state in both the tetragonal and the cubic average structures suggests that onset temperature of the ferroelectric state in the system is decoupled with the temperature associated with the crystal structures changes. In view of centrosymmetric structures at the global length scale, the appearance of ferroelectric state can be rationalized in terms of freezing of localized polar clusters as in relaxor ferroelectrics. Further, though the global structural distortion and the ferroelectric state are decoupled in the first approximation, the stabilization of the antiferrodistortive phase above room temperature is likely to affect the polarization values. First-principles studies have shown that AFD instabilities associated with octahedral tilting have the tendency to suppress the ferroelectric state in perovskites.[32] The decrease in remnant polarization with increasing Pr content, as observed in Fig. 4 of Ref. 17, may be attributed to the intervention of the AFD phase. The other likely explanation for the decrease in the polarization value could be increase in the dielectric loss with increasing the Pr content since more defect formation is likely to take place as the concentration of the hetrovalent Pr ions, which can exist in both the +3 and +4 states, increases. However, a perusal of the hysteresis loop, mentioned above, suggests that though the absolute value of polarization is low for x=0.075, the shape of the hysteresis loop suggests a relatively low lossy dielectric as compared to x=0.025, thereby suggesting that the AFD phase has a role to play in decreasing the polarization value of the system.

*rajeev@materials.iisc.ernet.in

[1] A. Bruce and R. Cowley, Adv. Phys. **29**, 219 (1980).
[2] J. F. Scott, Rev. Mod. Phys. **46**, 83 (1974).
[3] K. A. Müller and H. Burkard, Phys. Rev. B **19**, 3593 (1979).
[4] G. A. Samara and B. Morosin Phys. Rev. B **8**, 1256 (1973).
[5] H. Uwe and T. Sakudo, Phys. Rev. B **13**, 271 (1976).
[6] P. A. Fleury and J. M. Worlock, Phys. Rev. **174**, 613 (1968).
[7] J. Hemberger, M. Nicklas, R. Viana, P. Lunkenheimer, A. Loidl, and R. Böhmer, J. Phys.: Condens. Matter **8**, 4673 (1996).
[8] J. G. Bednorz and K. A. Müller, Phys. Rev. Lett. **52**, 2289 (1984).
[9] V. V. Lemanov, E. P. Smirnova, P. P. Syrnikov, and E. A. Tarakanov, Phys. Rev. B **54**, 3151 (1996).
[10] V. V. Lemanov, Phys. Solid State **39**, 1468 (1997).
[11] M. Itoh, R. Wang, Y. Inaguma, T. Yamaguchi, Y.-J. Shan, and T. Nakamura, Phys. Rev. Lett. **82**, 3540 (1999).
[12] R. Ranjan, D. Pandey, and N. P. Lalla, Phys. Rev. Lett. **84**, 3726 (2000).
[13] Chen Ang, Zhi Yu, P. Lunkenheimer, J. Hemberger, and A. Loidl, Phys. Rev. B **59**, 6670 (1999).
[14] N. A. Pertsev, A. K. Tagantsev, and N. Setter, Phys. Rev. B **61**, R825 (2000).
[15] J. H. Haeni, P. Irvin, W. Chang, R. Uecker, P. Reiche, Y. L. Li, S. Choudhury, W. Tian, M. E. Hawley, B. Craigo, A. K. Tagantsev, X. Q. Pan, S. K. Streiffer, L. Q. Chen, S. W. Kirchoefer, J. Levy, and D. G. Schlom, Nature (London) **430**, 758 (2004).
[16] I. A. Kornev and L. Bellaiche, Phase Transitions **80**, 385 (2007).
[17] A. Durán, E. Martínez, J. A. Díaz, and J. M. Siqueiros, J. Appl. Phys. **97**, 104109 (2005).
[18] R. Ranjan and R. Hackl, A. Chandra, E. Schmidbauer, D. Trots, and H. Boysen, Phys. Rev. B **76**, 224109 (2007).
[19] R. Ranjan, R. Garg, R. Hackl, A. Senyshyn, E. Schmidbauer, D. Trots, and H. Boysen, Phys. Rev. B **78**, 092102 (2008).
[20] A. Durán, F. Morales, L. Fuentes, and J. M. Siqueiros, J. Phys.: Condens. Matter **20**, 085219 (2008).
[21] L. E. Cross, Ferroelectrics **76**, 241 (1987).
[22] G. A. Samara, J. Phys.: Condens. Matter **15**, R367 (2003).

[23] J. Rodrigues-Carvajal "FULLPROF. A Rietveld Refinement and Pattern Matching Analysis Program," Laboratoire Leon Brillouin (CEA-CNRS) France.
[24] A. M. Glazer, Acta Crystallogr., Sect. B: Struct. Crystallogr. Cryst. Chem. **28**, 3384 (1972).
[25] A. M. Glazer, Acta Crystallogr., Sect. A: Cryst. Phys., Diffr., Theor. Gen. Crystallogr. **31**, 756 (1975).
[26] C. J. Howard and H. T. Stokes, Acta Crystallogr., Sect. A: Found. Crystallogr. **61**, 93 (2005).
[27] R. Ranjan, D. Pandey, V. Siruguri, P. S. R. Krishna, and S. K. Paranjpe, J. Phys.: Condens. Matter **11**, 2233 (1999).
[28] R. Ranjan, A. Agrawal, A. Senyshyn, and H. Boysen, J. Phys.: Condens. Matter **18**, L515 (2006); **18**, 9679 (2006).
[29] R. Ranjan, Ragini, S. K. Mishra, D. Pandey, and B. J. Kennedy, Phys. Rev. B **65**, 060102(R) (2002).
[30] D. M. Hatch, H. T. Stokes, R. Ranjan, S. K. Ragini, Mishra, D. Pandey, and B. J. Kennedy, Phys. Rev. B **65**, 212101 (2002).
[31] R. Ranjan and D. Pandey, J. Phys.: Condens. Matter **13**, 4251 (2001).
[32] W. Zhong and D. Vanderbilt Phys. Rev. Lett. **74**, 2587 (1995).